Scenarios of earthquake-generated tsunamis for the Italian coast of the Adriatic Sea

MARA MONICA TIBERTI[1], STEFANO LORITO[1], ROBERTO BASILI[1], VANJA KASTELIC[1,2], ALESSIO PIATANESI[1] AND GIANLUCA VALENSISE[1]

[1]*Istituto Nazionale di Geofisica e Vulcanologia, Sezione di Sismologia e Tettonofisica, Via di Vigna Murata 605, 00143 Rome, Italy.*

[2]*University of Ljubljana, Faculty of Natural Sciences and Engineering, Department of Geology, Aškerčeva 12, 1000 Ljubljana, Slovenia*

Abbreviated title: Tsunamis scenarios in the Adriatic Sea.

Corresponding author:
Mara Monica Tiberti
Istituto Nazionale di Geofisica e Vulcanologia, Sezione di Sismologia e Tettonofisica, Via di Vigna Murata 605, 00143 Rome, Italy
E-mail: tiberti@ingv.it
Phone: +39 06 51860443

Citation: Tiberti, M. M., S. Lorito, R. Basili, V. Kastelic, A. Piatanesi and G. Valensise (2008) - *Scenarios of earthquake-generated tsunamis in the Adriatic Sea*. PAGEOPH 165, 11/12, in press, doi: 10.1007/s00024-008-0417-6.

Abstract - We calculated the expected impact on the Italian coast of the Adriatic Sea of a large set of tsunamis resulting from potential earthquakes generated by major fault zones. Our approach merges updated knowledge on the regional tectonics and scenario-like calculations of expected tsunami impact.

We selected six elongated potential source zones. For each of them we determined a Maximum Credible Earthquake and the associated Typical Fault, described by its size, geometry and kinematics. We then let the Typical Fault float along strike of its parent source zone and simulated all tsunamis it could generate. Simulations are based on the solution of the nonlinear shallow water equations through a finite-difference technique. For each run we calculated the wave fields at specified simulation times and the maximum water height field (above mean sea level), then generated travel-time maps and maximum wave height profiles along the target coastline. Maxima were also classified in a three-level code of expected tsunami threat.

We found that the southern portion of Apulia facing Albania and the Gargano promontory are especially prone to the tsunami threat. We also found that some bathymetric features are crucial in determining the focalization-defocalization of tsunami energy. We suggest that our results be taken into account in the design of early-warning strategies.

Key words: Tsunamis, Adriatic Sea, seismotectonics, active faulting, seismic hazard, tsunami hazard

1. Introduction

The Adriatic Sea is an elongated basin stretching NW-SE in the central Mediterranean Sea (**Figure 1**). It has been struck several times by tsunamis (e.g.: Ambraseys, 1962; Caputo and Faita, 1984; Papazachos and Dimitriu, 1991; Soloviev et al, 2000; Maramai et al., 2007; Tinti et al., 2007; see also Paulatto et al., 2007 for a complete review), most often along the coasts of the Gargano promontory (De Martini et al., 2003; Tinti et al., 2004). The northwestern portion of the Adriatic basin is also the most vulnerable because of its large low-topography coastal area extending for over 150 km. This area also hosts the city of Venice, that is particularly to vulnerable to sea-level rise. From the regional tectonics standpoint, the Adriatic Sea falls in the middle of the Adria plate, that is being pushed by Africa northward against stable Europe. Overall, Adria is affected by active compression and overridden by thrust belts all around.

The purpose of this work was to assess systematically the potential threat posed by earthquake–generated tsunamis on the Italian coastline of the Adriatic Sea, following the approach proposed by Lorito et al. (2008). To this end, we first compiled a database of potentially-tsunamigenic earthquake faults, then used them as input in the preparation of scenarios of maximum water height (above mean sea level) based on numerical simulations of tsunami propagation. Potential tsunami sources were selected from the seismogenic sources listed in version 3.0.4 of the Database of Individual Seismogenic Sources (DISS Working Group, 2007; Basili et al., 2008), adapted to the modeling needs and integrated with additional data, particularly for the eastern side of the basin.

Our scenarios supply at-glance information of the expected tsunami impact onto the target coastline and can be progressively updated as knowledge on earthquake sources advances. As such, our approach can be easily converted into an application program for disaster prevention whose results can be handed out to a variety of stakeholders, such as civil protection agencies or land-use

planners. Similar approaches have been independently developed, for example, for Australia and New Zealand by Burbidge and Cummins (2007) and Power et al. (2007), respectively. Using a different approach, Paulatto et al. (2007) studied the tsunami potential of Adriatic Sea seismic sources adopting two fault locations for each selected source zone.

The results of our work include the determination of the maximum water height along 2100 km of the Adriatic Italian coastline calculated for six source zones located inside or very close to the Adriatic Sea. These results were compared with the threat posed by tsunamis generated in the Hellenic Arc source zone (Lorito et al., 2008), i.e. the source of the biggest tsunamis generated outside the basin with the capability to hit our target coastline. All profiles of maximum water heights are given in aggregated form together with averages and standard deviations. Maxima were also classified in a three-level code of expected tsunami threat. Finally, we explored the role of specific bathymetric features in controlling the focalization-defocalization of tsunami energy.

2. Method

To assess the potential threat posed by earthquake-generated tsunamis in the Adriatic Sea we adopted the method developed by Lorito et al. (2008). We systematically carried out a number of simulations for all source zones that can possibly affect the target coastlines. A Source Zone (SZ) includes an active tectonic structure at regional scale that is made up of a number of individual fault segments, each one capable of releasing a significant earthquake. For each SZ we identified a Maximum Credible Earthquake (MCE) and an associated Typical Fault (TF). We let the TF float along the entire SZ and computed a tsunami scenario at regular intervals. To assess the MCE for each SZ we selected the largest earthquake that has ever occurred in that zone and for which there exists, or is possible to obtain, a reliable magnitude estimation. The TF is defined by parameters

that must comply with both the seismological properties of the MCE and the tectonic properties of its parent SZ. To estimate them we largely relied on published data, and particularly on those made available in the DISS database (DISS Working Group, 2007; Basili et al., 2008). Strike, dip and rake were slightly adjusted as needed to account for the internal geometric variations of the SZ at each position of the TF. The amount of slip was derived from the seismic moment of the MCE, using the formulations by Kanamori and Brodsky (2004). Steps were taken at one or half fault length to guarantee a sufficient spatial sampling of the tsunamigenic structure. At each new position the TF was made to release its MCE by uniform slip over the entire fault plane. The initial seawater elevation associated with the earthquakes generated by the floating TF was assumed equal to the coseismic vertical displacement of the sea bottom computed according to Okada's (1985, 1992) formula. Rupture was assumed to be instantaneous, and the initial velocity field was assumed to be identically zero. For the numerical modeling of the tsunami propagation we used the nonlinear shallow water equations that were solved numerically by means of a finite difference method on a staggered grid (Mader, 2001). We set the boundary conditions as pure wave reflection at the solid boundary, by setting to zero the velocity component perpendicular to the coastline. Full wave transmission was set at the open boundary (open sea). The sea-floor topography was taken from the ETOPO2 bathymetric dataset (Smith and Sandwell, 1997), that we oversampled at 0.5 arcmin to achieve a sufficient sampling of the wave features. We fixed a minimum depth of 10 meters, then modified all shallower bathymetry accordingly. Our simulation domain is 9° to 23° longitude E, and 30° to 46° latitude N.

We performed a distinct numerical experiment for each fault position in each SZ for a total of 129 runs. From each simulation we extracted the maximum water height above sea level (HMAX) profiles along the Adriatic coasts of Italy. The HMAX was calculated at the points adjacent to the coastline, that is at a fixed water depth of 10 meters. The HMAX values along the target coastline were then grouped according to the causative source zone. For each group we then

calculated the absolute maximum, the average, and the standard deviation of the HMAX values. Finally, we set three HMAX thresholds at 0.05, 0.5, and 1.0 m and coded the different levels of threat as *marine*, *land* and *severe land threat*, respectively. Allen and Greenslade (2008) pointed out that the practical use of the threat levels requires much caution because the local effects of a tsunami can be precisely described only through fine-scale inundation models. In addition to being computationally very demanding, this approach is not feasible because inundation models rely on fine-scale bathymetry data that are currently not available for the entire coast under investigation (see also Lorito et al. 2008). Nevertheless the HMAX represents an average coastal level that is certainly appropriate for comparing risk levels and for tsunami preparedness, provided that a *caveat* is included specifying that the wave height can be locally higher.

3. Tsunamigenic source zones in the Adriatic Sea

The Adriatic Sea is almost completely surrounded by active fold-and-thrust belts and strike-slip faults (**Figure 1**). Frequent earthquakes occur along these well-known fault zones, most of which run close to the coastlines or in the open sea and are thus potential sources for tsunamis. The largest earthquakes (M>7) occurred near the eastern margin of the central Adriatic Sea, along the Montenegro portion of the Dinaride-Albanide chain, and at the southern end of the basin near the Ionian Islands along the Kefallonia-Lefkada right-lateral shear zone. Most of the remaining structures exhibit a potential for earthquakes of magnitude 6≤M≤7, thereby holding a significant tsunamigenic potential.

This section describes the local tectonic setting of the six selected Source Zones grouped into four major tectonic domains. The reasoning followed to define the Typical Fault (TF) of each zone will also be illustrated.

3.1. Dinarides, Albanides and Hellenides

A contractional belt longer than 1,000 km runs along the eastern margin of the Adriatic Sea from the southern Alps, to the north, to the Kefallonia-Lefkada Fault, to the south (**Figure 1**). This fold-and-thrust belt is usually split into three different domains named Dinarides, Albanides and Hellenides, respectively from north to south, that started forming as a consequence of subduction of Adria under the European plate. Adria acts as an indenter pushing northward into stable Europe (e.g. Aljinović et al., 1990; Prelogović et al., 1995; Herak, 1999). GPS data document compressional strain across the chain at a rate of about 30 nanostrain/yr (Hollenstein et al., 2003; Serpelloni et al., 2005). Stronger earthquakes mostly concentrate in the Albanides and Hellenides. The outer portion of these chains is partly located offshore and characterized by numerous thrust fronts that all seem to be currently active. Available focal mechanisms indicate predominant SW-NE shortening (Papazachos et al., 1999); reverse faulting earthquakes dominate (Vannucci et al., 2004; Pondrelli et al., 2006).

Croatia. The Dinarides is a wide NW-SE fold-and-thrust belt stretching from southwestern Slovenia to Croatia along the Adriatic coast (**Figure 1**). The Dinaric accretionary prism is dominated by NW-SE trending, NE dipping thrust faults (Mamužić, 1975; Ivanović et al., 1976; Herak, 1991, 1999) whose geometry is well imaged in seismic profiles and constrained by gravity surveys (**Figure 2a**; Skoko et al., 1987; Aljinović et al., 1990; Lawrence et al., 1995; Prelogović et al., 1995). In the southern and central parts of the Dinarides the active thrust front lies offshore and is blind along most of its length (Tari-Kovačić and Mrinjek, 1994; Herak et al., 2005). The amount of shortening and the hanging-wall displacement increase towards the NE, where the faults become surface-breaking (Kuk et al., 2000; Herak et al., 2005). Moving towards the NW, fault planes become steeper and exhibit more oblique to dextral strike-slip kinematics (Prelogović et al., 1995).

GPS studies show shortening rate across the central Dinarides of few millimeters per year (Battaglia et al., 2004; Grenerczy et al., 2005). Earthquake focal mechanisms show thrusting on NE-dipping faults at shallow to medium depth in the Dinarides and oblique to dextral-strike slip motion on steeper NE-dipping planes in the northern Adriatic (Herak et al., 1995; Ivančić et al., 2006). The average orientation of compression in the Dinaric region is N-S, varying from N15º to N340º (Herak et al., 1995; Prelogović et al., 1999, 2003), also consistent with GPS data. Bennett et al. (2007) used regional GPS data to model a N77°W oriented thrust fault that accommodates the modern stress field in the southern Dinarides.

Based on the geometry, kinematics, and spatial distribution of individual faults and on data on the associated instrumental and historical earthquakes, we have chosen to split the Dinarides into two source zones. One running close to the coast of mainland Croatia (**Figure 1**); the other located offshore almost in the middle of the Adriatic Sea (**Figure 1**).

The geometry and depth of the typical fault of the Coastal Croatia SZ (**Table 1**) were taken from published seismic profiles and analyses of instrumental earthquakes. From south to north, the strike of the typical fault varies by nearly 40° from NW-SE to NNW-SSE; in its turn, the rake varies from almost pure thrusting to dextral oblique thrusting. The strongest earthquake generated by the Dinaric coastal source zone is the M_L 6.1, 11 January 1962 Makarska earthquake that was also followed by a tsunami (Herak et al., 2001). Other earthquakes associated with this source zone are the 2 July 1898, I_0 = IX, Split; 29 December 1942, M_L 6.0, Imotski (Kuk et al., 2000); and 5 September 1996, M_L 6.0, Ston (Markušić et al., 1998). As the 1962 earthquake is the largest known event associated with this source zone, we chose M_W 6.1 as the magnitude of its MCE.

The Offshore Croatia SZ (**Table 1**) comprises a blind thrust faulting system. The strike of the typical fault changes from N320° to N290° from south to north whereas the rake changes from pure thrusting to oblique slip. The largest event recorded in the past 20 years is the 29 March 2003, M_W 5.6 earthquake, located near the island of Jabuka (Herak et al., 2005). Instrumental and

historical catalogues locate the 30 November 1934, M_L 5.6 event in the northwestern part of this source zone; Kuk et al. (2000) also place in the same epicentral region a disastrous event in 361 AD. Even if known earthquakes do not exceed M 5.6, we adopted the value of M_W 6.0 for the MCE because reports of the 361 AD earthquake hint at a larger magnitude than that of the more recent instrumental event.

Montenegro. This portion of the chain runs NW-SE parallel to the coast just offshore Montenegro and is narrower than its own northern and southern prolongations (**Figure 1**). It is made up by fewer major structures than the rest of the chain, but these structures are bigger and more tightly imbricated. The outermost thrust front lies about 20 km off the coast (**Figure 2c**; e.g. Dragasevic, 1983; Picha, 2002).

The area is currently characterized by moderate shallow instrumental earthquakes, but a number of strong events ($M_W \geq 7.0$) are listed in the historical catalogue compiled by Papazachos and Papazachou (1997). The largest well-known earthquake (M_W 7.1) occurred on 15 April 1979 off the coast of southern Montenegro (Console and Favali, 1981), and was probably generated by the most external thrust (Benetatos and Kiratzi, 2006). It also generated a tsunami (e.g.: Bedosti and Caputo, 1986; see also Paulatto et al., 2007 and references therein). Most earthquakes in this zone, including the 1979 event, exhibit reverse focal mechanisms with NW-SE fault planes (Vannucci et al., 2004; Benetatos and Kiratzi, 2006; Pondrelli et al., 2006), overall suggesting compression with P-axes oriented roughly N230º (Papazachos et al., 1999). The average strike and rake from focal mechanisms are consistent with plate motion vectors derived from GPS data and with the orientation of thrust fronts.

We placed the Montenegro SZ (**Table 1**) on the main and most external of the thrust fronts, which has the largest potential of generating tsunami and is thought to be responsible for the 1979 earthquake. As for the MCE we adopted M_W 7.2 based on the maximum magnitude assessment

given by Aliaj et al. (2004) for the Lezha-Ulqini area, which includes the majority of the Montenegro SZ. We derived strike, dip, and rake from focal mechanisms and from the average geometry of the thrust faults as revealed by seismic reflection profiles.

Albania - Northern Greece. In the southern Adriatic Sea, the submerged edge of the Apulia platform acts as an indenter in the European plate. Here continental collision creates a series of NW-SE thrusts fronts involving the Apulian platform itself (**Figure 1**), occasionally interrupted by NE-SW strike-slip faults. Seismic profiles image the sole-thrust at about 10 km depth (**Figure 2b**; e.g.: Argnani et al., 1996; Sulstarova et al., 2000; Ballauri et al., 2002; Finetti and Del Ben, 2005; Aliaj, 2006; Graham Wall et al., 2006).

The Albania offshore is characterized by shallow instrumental seismicity with many 4<M<5 earthquakes (Duni et al., 2003), but a number of larger events (up to M_W 6.8) are reported by historical catalogues (e.g. Papazachos and Papazachou, 1997). The offshore of northern Greece is also characterized by shallow seismicity, nonetheless events in the magnitude range 6 to 7 are frequent. The largest known event took place near Kerkira Island on 5 February 1786 and had an estimated M_W 7.0. Another large earthquake (M_W 6.8) is thought to have occurred near Kerkira on 20 February 1743 (Papazachos and Papazachou, 1997; see also Guidoboni et al., 2007 for a complete review). Most earthquakes exhibit reverse focal mechanisms over NW-SE planes both in Albania and northern Greece (Vannucci et al., 2004; Pondrelli et al., 2006). Subhorizontal compression with P-axes from focal mechanisms trending 230-240º dominates the area (Papazachos et al., 1999); the average strike and rake from focal mechanisms are consistent with plate motion vectors derived from GPS data and with the orientation of thrust fronts.

We identified the Albania - Northern Greece SZ (**Table 1**) as made of three segments that cover the set of thrust fronts having the highest potential for tsunami generation (**Figure 1**). As for the MCE we adopted the 1786 Kerkira Island event. A M_W 7.0 is also the maximum expected

magnitude estimated by Aliaj et al. (2004) for this area. Similarly to the Montenegro SZ, we derived strike, dip, and rake from focal mechanisms and from the average geometry of the thrust faults as detected on seismic reflection profiles.

3.2. Northern Apennines

The Apennines is a fold and thrust belt running all along the Italian peninsula. The northern Apennines orogenic wedge grew and migrated throughout the Neogene as a response to the NE-ward roll-back of a retreating slab at the western edge of the Adria plate (e.g. Royden et al., 1987 Doglioni, 1991). The most external thrust structures are known from seismic exploration data and are located offshore beneath a cover of Early Pliocene to Quaternary synorogenic deposits (**Figures 1** and **2d**; Casero et al., 1990; Del Ben, 2002; Franciosi and Vignolo, 2002; Scrocca et al., 2007).

The shortening rate across the thrust belt during the whole orogenic process is estimated at ~2.9 mm/yr (Basili and Barba, 2007, and references therein). Because of the limited number of permanent stations available, GPS data on strain rates for this area are scarce and not yet reliable; however they do indicate shortening at a few mm/yr across the northern Adriatic (Zerbini et al., 2006). In addition, geomorphic evidence for active growth above individual blind thrusts running along the coast has provided a slip rate of 0.24-0.36 mm/yr (Vannoli et al., 2004). Available focal solutions show NE-SW compression at shallow depth, consistent with the geometry of the thrusts detected in seismic profiles (Piccinini et al., 2006; Lavecchia et al., 2007; Meletti et al., 2008).

We identified a long portion of the coastal and offshore thrusts as the Northern Apennines SZ (**Table 1**). The largest known event occurred on 30 October 1930 on the coast nearby Senigallia and had an estimated magnitude of M_W 5.9. This event was followed by a small tsunami (Boschi et al., 2000). However, the 1930 earthquake is probably not the largest to have ever occurred in the area, as geological and geomorphic data from an area about 30 km to the NW indicate the presence of a fault whose size is compatible with earthquakes up to M_W 6.1 (DISS Working Group, 2007).

Although there is no known historical earthquake associated with this fault, we sized the TF of this source zone on the basis of geological evidence as this represents the worst case scenario. The eastern boundary of the source zone follows the pattern of the domain that according to Scrocca (2006) has been affected by contractional deformation during the Late Quaternary.

3.3. Apulia

The southern part of the Apulian foreland is characterized by a number of right-lateral E-W striking shear zones (**Figure 1**). These tectonic structures extend westward below the outer edge of the Apennines orogenic wedge and eastward into the Adriatic Sea. Most of them probably started forming during the Mesozoic under a different tectonic setting as left-lateral kinematics is documented by structures with a long deformation history, but according to the majority of workers their most recent reactivation is dominantly right-lateral (Argnani et al., 1993; Bosellini et al., 1993; Chilovi et al., 2000; Di Bucci and Mazzoli, 2003; Valensise et al, 2004). The northernmost shear zone, known as Tremiti Line, is thought to represent the effect at shallow crustal depths of a lithospheric tear in the Adria microplate (Doglioni et al., 1994). A few kilometers to the south of the Tremiti Line, the Molise-Gondola shear zone, which includes the Mattinata fault, shows evidence for recent dextral strike-slip activity in the offshore (Di Bucci et al, 2007; Ridente et al., 2008).

The present-day stress field of this source zone exhibits NE-SW compression that appears to be a direct result of the Africa-Europe convergence (e.g.: Noquet and Calais, 2004; Serpelloni et al., 2007). Focal mechanisms mostly consist of dextral strike-slip faulting on subvertical planes at depths of 10-25 km (Pondrelli et al., 2004; Vannucci et al., 2004; Milano et al., 2005; Del Gaudio et al., 2007). The western portion of the Molise-Gondola shear zone is responsible for the 31 October and 1 November 2002, M_W 5.7 Molise earthquakes (Valensise et al., 2004; Chiarabba et al., 2005). Historical and instrumental seismicity data suggest the presence of similar shear zones both to the north and to the south of the Molise-Gondola (Fracassi and Valensise, 2007; Meletti et al., 2008).

The largest known earthquake of the Apulian foreland is the 30 July 1627, M_W 6.7 Gargano event (Gruppo di lavoro CPTI, 2004). It was followed by a tsunami that severely affected the northern coast of the Gargano Promontory (Tinti and Piatanesi, 1996; Boschi et al., 2000; Tinti and Armigliato, 2003), where geological evidence for recurrent tsunamis is found in coastal deposits (De Martini et al., 2003). We have chosen the Molise-Gondola shear zone as a sample structure for the whole set of E-W faults that affect this region because it is the best documented structure, especially in the offshore, and adopted it as the Apulia SZ (**Table 1**). The size of the 1627 earthquake was adopted as its MCE; its causative source from DISS Working Group (2007) was taken as typical fault for this shear zone.

3.4. Kefallonia-Lefkada

The Kefallonia-Lefkada Fault marks the boundary between the NNE-directed subduction of the Africa oceanic lithosphere beneath the Aegean continental lithosphere to the south and the continental collision between the Adriatic and European plates to the north (**Figure 1**). South of the Kefallonia-Lefkada alignment the rate of convergence between the African and Aegean plates is ~4-5 cm/yr and observed GPS velocities are the fastest of the entire Mediterranean basin (Kahle et al., 2000; McClusky et al., 2000), whereas north of it they decrease rapidly. As a result, inferred strain rates vary from more than 100-200 nanostrain/yr in the Hellenic Arc to about 30 nanostrain/yr in the Hellenides chain (Kahle et al., 2000; Hollenstein et al, 2003). The Kefallonia-Lefkada Fault thus accommodates a deformation of at least 100 nanostrain/yr (Kahle et al., 1998; Hollenstein et al, 2006). GPS data also indicates right-lateral relative motion across the shear zone at ~4 cm/yr, even if earthquakes account for only about 50% of that value (Kahle et al., 1996).

The Kefallonia-Lefkada Fault is one of the most seismically active areas in the Mediterranean and is largely characterized by strike-slip earthquakes (Papazachos et al., 1998; Vannucci et al., 2004). In 1983 a M_W 7.0 earthquake with a transpressional mechanism occurred on

the southern portion of the zone (Papazachos and Papazachou, 1997; Louvari et al., 1999). The largest known event in this area is the 12 August 1953, M_W 7.3 Kefallonia earthquake that caused ~0.5 m of vertical displacement testified by raised shorelines (Pirazzoli et al., 1994; Stiros et al., 1994). Louvari et al. (1999) associate this earthquake with the southern segment of the Kefallonia-Lefkada strike-slip fault.

We identified as the Kefallonia-Lefkada SZ (**Table 1**) the entire fault and adopted the size of the 1953 event (M_W 7.3) as the MCE, consistent with the maximum magnitude reported for the Kefallonia zone by Papaioannou and Papazachos (2000). We constrained the depth of this SZ based on the hypocentral distributions from various workers (up to 20 km). Strike, dip and rake were also based on data from various workers who analyzed the instrumental seismicity (Papazachos et al., 1998; Louvari et al., 1999); its kinematics is consistent with the GPS velocity field by Cocard et al. (1999).

4. Modeling results

We analyzed the tsunami impact expected on the Adriatic coasts of Italy as a result of earthquakes generated in each of six independent SZs. All tsunamis generated by a single SZ were grouped together. The corresponding HMAXs expected along the Adriatic coastline of Italy are shown as profiles of their maximum, average and average plus one standard deviation, respectively (**Figure 3**). Abscissa values are distances along the coastline and increase from south to north from an arbitrarily chosen starting point (**Figure 4**); since the true length of coastlines depends on the yardstick used, these are not intended to be accurate distances but rather a practical way to map the HMAXs values along the coastline. We also emphasized the threat level by color coding the background of each diagram. The use of such color codes is quite a common practice and a similar

approach is routinely adopted for tsunami warnings and advisory by the Japan Meteorological Agency (http://www.jma.go.jp/en/tsunami/). We decided to adopt a three-color code: yellow for *marine threat*, corresponding to 0.05 m < HMAX < 0.5 m; orange for *land threat*, corresponding to 0.5 m < HMAX < 1 m; red for *severe land threat*, corresponding to HMAX > 1 m. This choice is coherent with the approach followed by Allen and Greenslade (2007), who proposed a three-level stratified warning method and set a threshold of 0.5 m between *marine* and *land threat* based on Whitmore (2003).

4.1. Croatia, Montenegro, Albania, and Northern Greece

Our calculations show that the offshore Croatia SZs pose a rather low threat to a ~700 km-long stretch of the Adriatic coast of Italy from the northern edge of the Gargano promontory to north of Ancona (**Figure 3a**). Here the level of maximum HMAXs (black line) enters the yellow zone by 0.1 m at the most, hence exceeding the lower threshold of the *marine threat* level. Conversely the average HMAX (blue line) always lies below the this level. The difference between the maximum and average values is almost one order of magnitude at some locations, and the standard deviation is relatively high (green line). This may be the evidence that, depending on the relative position of the fault with respect to the coast, the tsunamis following each single earthquake generated by the floating fault have mainly local effects. It is also likely that the main contribution to the maximum values is brought by the source zone facing the coasts of Italy, whereas tsunamis generated in the Coastal Croatia SZ are shielded by the Dalmatian Islands (**Figure 1** and **4**).

The Montenegro SZ revealed a tsunamigenic potential beyond the attention level, i.e. over the lower bound of *marine threat*, almost everywhere on the Adriatic coast of Italy (**Figure 3b**), and consistently inside the *marine threat* band from about the 150 km position in Apulia to just north of Ancona. *Land threat* (orange background) is to be taken into account for a ~550 km-long stretch running along the Apulian coast from the 200 km position to north of the Gargano promontory. The

Gargano itself is exposed to a *severe land threat* level, as shown in **Figure 3b**, where the peak of the maximum values (black line) is almost two meters high, thereby largely entering the red code zone.

The Albania - Northern Greece SZ (**Figure 3c**) poses a threat comparable to that of Montenegro. The *marine threat* level is reached on the entire coast stretch from Apulia up to around Ancona, but the southern part of Apulia is exposed to *land* and even *severe land threat* involving a ~50 km-long stretch where the highest peak of maximum HMAX may exceed 1.5 m.

It is worth analyzing jointly the results we obtained for the Montenegro and Albania as they revealed a peculiar bathymetry-induced propagation effect due to the presence of the relatively deep South Adriatic Basin (**Figure 1**). **Figures 5a-c** show HMAX maps for the entire calculation domain. **Figures 5a** and **5b** show the propagation of the tsunamis generated by two earthquakes on the Montenegro SZ, whereas **Figure 5c** shows a tsunami generated by the Albania - Northern Greece SZ. The case of **Figure 5b** shows that the basin acts as a convex lens deflecting most of the propagating wave energy back to the Montenegro coast, thus limiting the height of the tsunami wave reaching the Apulian coast. This effect is predicted for faults located in the southernmost portion of the Montenegro SZ. Conversely, when the source fault is placed to the north of the South Adriatic Basin (**Figure 5a**) tsunami energy is focused towards the Gargano promontory at the basin edge. This is why the height of the narrow peak of the maximum values at ~650 km in **Figure 3b** is almost three times larger than the corresponding average value, and it is abundantly in the *severe land threat* band, whereas the threat to the adjacent coast to the south is only at the *land threat* level, with an average of less than a half of the tsunami wave height. At the southern end of the basin, the Albania - Northern Greece SZ again exceeds 1.0 m (**Figure 5c**), and poses a *severe land threat* to Apulia. In this case, the vicinity of the sources to the target coasts causes the maximum being about three times the average HMAX values (**Figure 3c**), meaning that the tsunami may be locally higher along the stretch of coast directly facing the source. This *severe land threat* peak is

slightly broader than that of the Montenegro SZ case, reflecting the fact that more than one source contributes to it as the fault floats.

4.2. Northern Apennines

The Northern Apennines SZ generally poses a low threat that can only locally be slightly higher but is always comparable to that of the Croatia offshore SZ. The affected portion of the Adriatic coasts of Italy is restricted to a ~750 km-long stretch from the northern side of the Gargano promontory to the south of the Po River delta (**Figure 3d**). The level of maximum HMAXs (black line) attains the *marine threat* zone from ~1050 to ~1400 km. Similarly to the Croatia SZ, the average (blue line) is significantly lower than the maximum HMAX. Near-field effects of the coastal sources again dominate, the main contribution to the maximum being brought by faults facing the coasts of Italy, whereas faults running farther offshore contribute relatively less (**Figure 1**). The peak at ~450 km could result from a focalization effect at the northern edge of the deeper South Adriatic Basin, as illustrated earlier for the Montenegro case.

4.3. Apulia

The typical fault floating along the Apulia SZ generates a series of tsunamis that may pose a *marine threat* (**Figure 3e**) along a stretch of coast extending from Bari (at 400 km) northward for ~500 km. Further north the lower *marine threat* threshold is exceeded only at scattered locations. Around the ~500 km position there seem to be only near-field effects, as revealed by the difference between maximum and average values. The highest peak is almost 0.5 m, just below the lower threshold of *land threat*, and occurs at ~640 km.

4.4. Kefallonia-Lefkada

The maximum HMAXs profile of the Kefallonia-Lefkada SZ (**Figure 3f**) features a quite narrow peak that starts in the *marine threat* band and then rises into the *land threat* band in the 40-140 km interval. Maximum height is ~0.9 m, almost at the lower threshold of the *severe land* threat band. The maxima curve then drops again while remaining in the *marine threat* band as far as a point at 640 km. North of the Gargano promontory the coast is free from serious threats. Conversely, the peak that almost reaches the *severe land threat* level is due to a bathymetric effect (**Figure 5d**). The shelf extending to the southeast of Apulia (**Figure 1**) acts as a wave-guide for tsunami propagation. It focuses the energy in a relatively narrow band thereby enhancing the wave height that reaches the southernmost tip of Apulia. This is the well understood continuous refraction and amplification phenomenon seen during the global propagation of the 26 December 2004 Sumatra-Andaman tsunami - just to mention a recent example - when the wave reached the Mid-Atlantic Ridge, which in turn efficiently transmitted the wave energy (Thomson et al., 2007). Another example of a similar phenomenon is the unexpectedly big damage suffered by the Crescent City harbor, California, on occasion of the 15 November 2006 Kuril islands earthquake (M_W 8.3) and tsunami. The damage was caused by a secondary wave that was reflected by a sea-mount and focused by the Mendocino escarpment and that arrived at Crescent City two hours after the main wave (Kowalik et al., 2008). Thus, despite the little vertical sea-floor displacement expected due to the strike-slip style of the causative fault, the Kefallonia-Lefkada SZ poses a significant threat to the coasts of Italy, which may be further increased by bathymetric amplification.

5. Discussion

We investigated the potential effects on the Italian coasts of the Adriatic Sea for all the earthquake source zones that are known to be capable of generating tsunamis. To this end we used an approach

that combines a detailed knowledge of the tectonic setting of the source zones with the evaluation of the tsunami impact onto the target coastline. This was done by introducing the concept of a typical fault that is sized after the maximum credible earthquake of the area and is let floating along its parent source zone.

Similar approaches for other tsunami-prone areas in the world are those of Burbidge and Cummins (2007) and Power et al. (2007). The first explored the effects onto the western coast of Australia for tsunamis generated by faults in three different positions along the Sunda Arc with two possible earthquake magnitudes (M_W 8.5 and 9.0). The second analyzed the impact onto New Zealand coasts of tsunamis generated in the South America subduction zone, exploring a range of possible earthquake magnitudes and obtaining results expressed in probabilistic terms.

By displaying the aggregated HMAX values all along target coastlines our method allows an easy comparison between the effects of different source zones and shows the relative level of tsunami threat for different stretches of the coast. The results of our modeling could also serve as input data for detailed studies on local effects, provided that finer bathymetry data are available. The purpose of our work is to provide an estimation of HMAX for an earthquake occurring at any position along a known source zone rather than just for a specific past earthquake. Historical tsunamis of the Adriatic Sea were recently reviewed by Paulatto et al. (2007), who also carried out simulations for a set of earthquakes in six potential source zones. Their approach, however, substantially differs from ours as the earthquake sets are defined considering three magnitude values and three depth values at two locations, inland and offshore, for each source zone; the results are then shown in terms of maximum water height and arrival time at selected localities.

Our predictions can be compared with limited historical accounts of tsunamis that occurred around the Adriatic basin:

- according to Guidoboni and Tinti (1988), the tsunami that followed the 1627 Gargano earthquake caused sea withdrawal of about 3 km at the mouth of the Fortore River (northern

side of Gargano) and an estimated run-up of 2-3 m in the town of Manfredonia (southern side of Gargano);

- according to contemporary newspapers, an anomalous high tide was observed in the Ancona harbor after the 1930 Senigallia earthquake. An American steamship broke the moorings and hit the docks. A tsunami intensity of 4 is attributed to this event in the Italian Tsunami Catalogue (Boschi et al., 2000; Maramai et al., 2007; Tinti et al., 2007);
- according to Soloviev et al. (2000), no tsunami followed the 1953 Kefallonia earthquake, even if previous publication based on press reports indicated the flooding of the port of Vathi (Lefkada Island). In any case, flooding of the port was ascribed to a local landslide and was hence not a direct effect of seafloor displacement;
- a minor disturbance was recorded at the tide gauge of Split following the 1962 Makarska earthquake (Herak et al, 2001);
- although Papazachos and Papazachou (1997) report that after the 1979 Montenegro earthquake a ship sank and several houses on the waterfront were taken off, at Boka Kotorska (Montenegro) the tide gauges recorded a sea wave of just 6 cm. Other disturbances were noticed at the tide gauges of Dubrovnik and Bari (Bedosti and Caputo, 1986; Soloviev et al., 2000).

For the Kefallonia, Makarska and Montenegro tsunamis our results show HMAX values greater than those reckoned by interpreting available historical data, in agreement with our aim at representing worst-case scenarios. The tsunamis following the Senigallia and Gargano earthquakes need further discussion. The Senigallia tsunami produced significant effects only in the harbor of Ancona. Even if an instrumental measure of tsunami effects in the harbor of Ancona does not exist, we cannot rule out that our simulation underestimates the wave height inside the harbor. This may be due to poor resolution of the bathymetry model at the harbor scale, and/or to local amplifications and resonance phenomena that are common in quasi-closed basins (e.g.: Kowalik et al., 2008). The Gargano tsunami is a case that, despite several studies, still presents unresolved issues. A major

inconsistency exists between the macroseismic field, that suggests an inland source, and the tsunami effects, that cannot be satisfactorily reproduced either by inland or offshore sources (Tinti and Piatanesi, 1996; Tinti and Armigliato, 2003). For this tsunamigenic source we estimated a maximum wave of about 0.5 m, comparable to the results of Tinti and Piatanesi (1996). One could invoke a contribution by a secondary source (e.g. a submarine landslide), but this option falls outside the scopes of our work.

To fully explore the significance of our results in terms of tsunami threat to the Italian coasts of the Adriatic Sea we used the results obtained by Lorito et al. (2008) for the Hellenic Arc SZ as a term of comparison. Their HMAXs (**Figure 6**) show that the Hellenic Arc SZ poses a *severe land threat* to southern Apulia; the threat drops progressively northward to the level of *land threat* first, then to *marine threat* north of the Gargano promontory, and finally to nearly no threat north of Ancona. Remarkably, even the propagation of tsunamis from the Hellenic Arc SZ into the Adriatic Sea is strongly influenced by the two bathymetric effects illustrated in the previous section. The first is the focalization along the ridge that conveys energy towards the southernmost tip of Apulia - resulting in a peak of more than 4 m in the HMAX profile (**Figure 6**) - similarly to what was illustrated for the Kefallonia-Lefkada SZ. The second is the shielding effect of the northern Adriatic by the South Adriatic Basin. This results in a deflection of most of the wave energy towards the coast of the southern Adriatic Sea and a consequent increased dissipation. Recall that a similar shielding effect has already been discussed for the Albania - Northern Greece and Montenegro SZs.

Figure 7 summarizes the HMAXs associated with all six SZs considered in this study. Although most of the sources generate waves well beyond the level of attention of the *marine threat* band, we found that only three SZs enter the *land threat* band. The first is the Kefallonia-Lefkada SZ (black line) which, despite its limited size and strike-slip style, poses a significant threat for a short reach of the coast due to the bathymetric focalization. The two most threatening SZs are the Albania -Northern Greece (magenta) and Montenegro (blue) SZs, which generate water heights that

locally exceed the *severe land threat* level. The threat posed by the Albania - Northern Greece SZ, however, is always lower than that posed by the Hellenic Arc (gray line) at the same coastal positions. Nevertheless, tsunami waves from the Albania - Northern Greece SZ reach the Italian coast in less than 30 minutes (**Figure 8a**), whereas waves from the Hellenic Arc take 50 to 90 minutes (Lorito et al., 2008), depending on the exact position of the fault source. This means that the time available to issue a warning or take countermeasures is much shorter in the case of the Albania - Northern Greece SZ. The threat posed by the Montenegro SZ exceeds that of the Hellenic Arc for a significant coastline length and the HMAX peak at ~640 km is the highest of all Adriatic source zones (**Figure 7**). However, the propagation of tsunamis from the Montenegro SZ to the coasts of Italy takes more than 50 minutes (**Figure 8b**), comparable with the minimum time needed for propagation from the Hellenic Arc.

The combination of expected HMAX values and propagation times will become especially useful in the design of early-warning systems if integrated with analyses of the Euro-Mediterranean seismic network performance (e.g. Olivieri and Scognamiglio, 2007) for different tsunamigenic source zones.

6. Conclusions

Following the approach proposed by Lorito et al. (2008) we defined a maximum credible earthquake and an associated typical fault for each of six source zones potentially threatening the Adriatic coasts of Italy with sizable tsunamis. For each of the zones we let a pre-defined typical fault float along the entire source zone and computed a tsunami scenario at regular intervals. We then aggregated the maximum water heights above the mean sea level of each source zone and performed calculations of their maxima, averages and standard deviations along the target Adriatic Sea coasts of Italy. We finally coded the resulting tsunami threat for three different levels defined as: *marine*, *land* and *severe land*, shown in yellow, orange and red respectively.

We found that the southern part of Apulia facing Albania and the Gargano promontory are the portions of the Adriatic coasts facing the largest tsunami threat (**Figure 4**). We also found that some bathymetric features are crucial in determining the focalization-defocalization of tsunami energy. Despite its expected strike-slip faulting style, the Kefallonia-Lefkada source poses a significant threat for the southernmost tip of Apulia due to energy focalization along a bathymetric ridge. A further significant result is that the northern part of the Adriatic coast, where the cities of Venice and Trieste are located, is generally safer than the southern part. Only the region south of the Po delta may suffer from tsunamis, also due to its intrinsic vulnerability to flooding resulting from the extremely flat topography.

We also compared the threat posed by the investigated sources to that associated with earthquake sources in the Hellenic Arc. We found that the latter is potentially more destructive than the former, although the effects of small local sources can outpace those of the Hellenic Arc sources at specific locations. This is partly due to bathymetric effects, which can either reduce or enhance the threat posed by sources falling at specific locations.

We believe our results can be a valuable guidance for designing early warning systems, assessing risk and planning land-use for the coasts of southern Italy.

Acknowledgments

This work was partly funded by the Italian Civil Defense through INGV-DPC Project S2 "Assessing the seismogenic potential and the probability of strong earthquakes in Italy", grants to RB and AP. MMT was supported by the project "Development of new technologies for the protection of the Italian territory from natural hazards" funded by the Italian Ministry of University and Research. SL was supported by the Italian Civil Defense. VK was supported by a research grant from the Slovene Human Resources Development and Scholarship Fund "Ad futura". The authors thank Umberto Fracassi for fruitful discussion about the tectonics of Apulia, Branislav Glavatovic for providing information on the seismotectonics of Montenegro, Vlado Kuk for providing information about Croatian earthquakes, and Davide Scrocca for insights into the tectonics of the northern Adriatic. We also acknowledge Kenji Satake and two anonymous reviewers for their precious comments and suggestions.

REFERENCES

Aliaj, S., The Albanian orogen: convergence zone between Eurasia and the Adria microplate, In The Adria Microplate: GPS Geodesy, Tectonics and Hazards (eds. Pinter N. et al.) (Springer, Netherlands 2006) pp.133-149.

Aliaj, S., Adams, J., Halchuk, S., Sulstarova, E., Peçi, V., and Muço, B. (2004), Probabilistic seismic hazard maps for Albania, 13th World Conference on Earthquake Engineering, Vancouver, B.C., Canada, August 1-6, Paper No. 2469.

Aljinović, B., Prelogović, E., and Skoko, D. (1990), Tectonic processes on the contact of the Adriatic Platform and the Dinarides in the area of the Northern Dalmatia, Conf. on mechanics of jointed and faulted rock, Inst. of Mech/Tech. Univ. of Vienna, Proc. A. A. Balkema, Rotterdam/Brookfield, 179– 182.

Allen, S. C. R., and Greenslade, D. J. M. (2007), Developing tsunami warnings from numerical model output, Nat. Hazards 46, 35-52, doi: 10.1007/s11069-007-9180-8.

Ambraseys, N. N. (1962), Data for the investigation of seismic sea waves in the Eastern Mediterranean, Bull. Seism. Soc. Am. 52, 895–913.

Argnani, A., Favali, P., Frugoni, F., Gasperini, M., Ligi, M., Marani, M., Matietti, G., and Mele, G. (1993), Foreland deformational pattern in the Southern Adriatic, Ann. Geofis. 36, 229–247.

Argnani, A., Bonazzi, C., Evangelisti, D., Favali, P., Frugoni, F., Gasperini, M., Ligi, M., Marani, M., and Mele, G. (1996), Tettonica dell'Adriatico Meridionale, Mem. Soc. Geol. It. 51, 227-237.

Ballauri, A., Bega, Z., Meehan, P., Gambini, R., and Klammer, W. (2002), Exploring in structurally complex thrust belt: Southwest Albania Case, AAPG Hedberg Conference, May 14-18, 2002, Palermo-Mondello (Sicily, Italy).

Basili, R., and Barba, S. (2007) Migration and shortening rates in the northern Apennines, Italy: implications for seismic hazard, Terra Nova 19, 462–468, doi: 10.1111/j.1365-3121.2007.00772.x.

Basili, R., Valensise, G., Vannoli, P., Burrato, P., Fracassi, U., Mariano, S., Tiberti, M. M., and Boschi, E. (2008), The Database of Individual Seismogenic Sources (DISS), version 3: summarizing 20 years of research on Italy's earthquake geology, Tectonophysics, 453, 20-43, doi:10.1016/j.tecto.2007.04.014.

Battaglia, M., Murray, M. H., Serpelloni, E., and Bürgmann, R. (2004), The Adriatic region: an independent microplate within the Africa-Eurasia collision zone, Geophys. Res. Lett. 31, L09605, doi:10.1029/2004GL019723.

Bedosti, B., and Caputo, M. (1986), Primo aggiornamento del catalogo dei maremoti delle coste italiane, Atti della Accademia Nazionale dei Lincei, Rendiconti Classe Scienze Fisiche, Matematiche, Naturali s.VIII, 80, 570–584.

Benetatos, C., and Kiratzi, A. (2006) Finite-fault slip models for the 15 April 1979 (Mw 7.1) Montenegro earthquake and its strongest aftershock of 24 May 1979 (Mw 6.2), Tectonophysics 421, 129–143.

Bennett, R.A., Hreinsdóttir, S., Buble, G., Bašić, T., Bačić, Ž., Marianović, M., Casale, G., Gendaszek, A., and Cowan, D. (2007), Eocene to present subduction of southern Adria mantle litosphere beneath the Dinarides, Geology 36, 3-6, doi: 10.1130/G24136A.1.

Boschi, E., Guidoboni, E., Ferrari, G., Mariotti, D., Valensise, G., and Gasperini, P. (eds.) (2000), Catalogue of strong italian earthquakes from 461 B.C. to 1997, Ann. Geofis. 43, with CD-Rom, 259 pp.

Bosellini, A., Neri, C., and Luciani, V. (1993), Platform margin collapses and sequence stratigraphic organization of carbonate slopes: Cretaceous-Eocene, Gargano Promontory, Terra Nova 5, 282-297.

Burbidge, D., and Cummins, P. (2007), Assessing the threat to Western Australia from tsunami generated by earthquakes along the Sunda Arc, Nat. Hazards 43, 319-331, doi:10.1007/s11069-007-9116-3.

Caputo, M., and Faita, G. (1984), Primo catalogo dei maremoti delle coste italiane, Atti Accademia Nazionale dei Lincei, Memorie Classe Scienze Fisiche, Matematiche, Naturali s. VIII, 17, 213–356.

Casero, P., Rigamonti, A., and Iocca, M. (1990), Paleogeographic relationships during Cretaceous between the Northern Adriatic area and the Eastern Southern Alps, Mem. Soc. Geol. It. 45, 807-814.

Chiarabba, C., De Gori, P., Chiaraluce, L., Bordoni, P., Cattaneo, M., De Martin, M., Frepoli, A., Michelini, A., Monachesi, A., Moretti, M., Augliera, G.P., D'Alema, E., Frapiccini, M., Gassi, A., Marzorati, S., Di Bartolomeo, P., Gentile, S., Covoni, A., Lovisa, L., Romanelli, M., Ferretti, G., Pasta, M., Spallarossa, D., and Zumino, E. (2005), Mainshocks and aftershocks of the 2002 Molise seismic sequence, southern Italy, J. Seismol. 9, 487–494.

Chilovi, C., De Feyter, A. J., and Pompucci, A. (2000), Wrench zone reactivation in the Adriatic Block: the example of the Mattinata Fault System (SE Italy), Boll. Soc. Geol. It. 119, 3-8.

Cocard, M., Kahle, H.-G., Peter, Y., Geiger, A., Veis, G., Felekis, S., Paradissis, D., and Billiris, H. (1999), New constraints on the rapid crustal motion of the Aegean region: recent results inferred from GPS measurements (1993–1998) across the West Hellenic Arc, Greece, Earth and Planetary Science Letters 172, 39–47.

Console, R., and Favali, P. (1981), Study of the Montenegro earthquake sequence (March–July 1979), Bull. Seism. Soc. Am. 71, 1,233–1,248.

Del Ben, A. (2002), Interpretation of the CROP M-16 seismic section in the Central Adriatic Sea, Mem. Soc. Geol. It. 57, 327-333.

Del Gaudio, V., Pierri, P., Frepoli, A., Calcagnile, G., Venisti, N., and Cimini, G.B. (2007), A critical revision of the seismicity of Northern Apulia (Adriatic microplate — Southern Italy) and implications for the identification of seismogenic structures, Tectonophysics 436, 9–35.

De Martini, P. M., Burrato, P., Pantosti, D., Maramai, A., Graziani, L., and Abramson, H. (2003), Identification of tsunami deposits and liquefaction features in the Gargano area (Italy): paleoseismological implication, Ann. Geophys.-Italy 46, 883-902.

Di Bucci, D., and Mazzoli, S. (2003), The October-November 2002 Molise seismic sequence (southern Italy): an expression of Adria intraplate deformation, J. Geol. Soc. London 160, 503-506.

Di Bucci, D., Ravaglia, A., Seno, S., Toscani, G., Fracassi, U., and Valensise, G. (2007), Modes of fault reactivation from analogue modeling experiments: Implications for the seismotectonics of the Southern Adriatic foreland (Italy), Quaternary International 171–172, 2–13.

DISS Working Group (2007), Database of Individual Seismogenic Sources (DISS), Version 3.0.4: A compilation of potential sources for earthquakes larger than M 5.5 in Italy and surrounding areas, http://diss.rm.ingv.it/diss.

Doglioni, C. (1991), A proposal for the kinematics modelling of the W-dipping subductions-possible application to the Tyrrhenian-Apennines system, Terra Nova 3, 423-434.

Doglioni, C., Mongelli, F., and Pieri, P. (1994), The Puglia uplift (SE Italy): An anomaly in the foreland of the Apenninic subduction due to buckling of a thick continental lithosphere, Tectonics 13, 1309-1321.

Dragašević, T. (1983), Oil geologic exploration in the Montenegro offshore in Yugoslavia, Nafta 7-8, 397-404.

Duni, L., Kuka N., and Dushi, E. (2003), Monitoring of seismicity in Albania, CSEM Newsletter n. 20, September 2003, 13-16, www.emsc-csem.org.

Finetti, I.R., and Del Ben, A., Crustal tectono-stratigraphic setting of the Adriatic Sea from new CROP seismic data, In CROP, Deep seismic exploration of the Mediterranean region (ed. Finetti I R.) (Elsevier, 2005) pp. 519-547.

Fracassi, U., and Valensise, G. (2007), Unveiling the sources of the catastrophic 1456 multiple earthquake: Hints to an unexplored tectonic mechanism in Southern Italy, Bull. Seismol. Soc. Am. 97, 3, 725-748, doi:10.1785/0120050250.

Franciosi, R., and Vignolo, A. (2002), Northern Adriatic foreland - a promising setting for the southalpine midtriassic petroleum system, EAGE 64th Conference & Exhibition — Florence, Italy, 27 - 30 May 2002.

Graham Wall, B.R., Girbacea, R., Mesonjesi, A., and Aydin, A. (2006), Evolution of fracture and fault-controlled fluid pathways in carbonates of the Albanides fold-thrust belt, Am. Ass. Petroleum Geologists Bull. 90, 1227-1249, doi:10.1306/03280304014.

Grenerczy, G., Sella, G., Stein, S., and Kenyeres, A. (2005), Tectonic implications of the GPS velocity field in the northern Adriatic region, Geophys. Res. Lett. 32, L16311, doi:10.1029/2005GL022947.

Gruppo di lavoro CPTI (2004), Catalogo Parametrico dei Terremoti Italiani, versione 2004 (CPTI04). INGV, Bologna (also available at: http://emidius.mi.ingv.it/CPTI04/).

Guidoboni E., Ferrari, G., Mariotti, D., Comastri, A., Tarabusi, G., and Valensise, G. (2007), CFTI4Med, Catalogue of Strong Earthquakes in Italy (461 B.C.-1997) and Mediterranean Area (760 B.C.-1500), INGV-SGA, available at http://storing.ingv.it/cfti4med/.

Guidoboni, E., and Tinti, S. (1988), A review of the historical 1627 tsunami in southern Adriatic, Sci. Tsunami Hazards 6, 11-16.

Herak, M.J. (1991), Dinarides. Mobilistic view of the genesis and structure, Acta Geologica 21, 35–117.

Herak, M.J. (1999), Tectonic interrelation of the Dinarides and the Southern Alps, Geologica Croatica 52, 83– 98.

Herak, M., Herak, D., and Markušić, S. (1995), Fault plane solutions for earthquakes (1956–1995) in Croatia and neighbouring regions, Geofizika 12, 43– 56.

Herak, D., Herak, M., Prelogović, E., Markušić, S., and Markulin, Ž. (2005), Jabuka island (Central Adriatic Sea) earthquakes of 2003, Tectonophysics 398, 167– 180.

Herak, M., Orlić, M., and Kunovec-Varga, M. (2001), Did the Makarska earthquake of 1962 generate a tsunami in the central Adriatic arcipelago?, J. of Geodyn. 31, 71-86.

Hollenstein, C., Kahle, H.-G., and Geiger, A., Plate tectonic framework and GPS-derived strain-rate field within the boundary zones of the Eurasian and African plates, In The Adria Microplate: GPS Geodesy, Tectonics and Hazards (eds. Pinter N. et al.) (Springer, Netherlands 2006) pp. 35-50.

Hollenstein, Ch., Kahle, H.-G., Geiger, A., Jenny, S., Goes, S., and Giardini, D. (2003), New GPS constraints on the Africa-Eurasia plate boundary zone in southern Italy, Geophys. Res. Lett. 30, 1935, doi:10.1029/2003GL017554.

Ivanović, A., Sakač, K., Marković, S., Sokač, B., Šušnjar, M., Nikler, L., and Šušnjara, A. (1976), Osnovna geološka karta SFRJ, list Obredovac, 1:100000, Inst. geol. istraž., Zagreb (1967), Savezni geol. zavod, Beograd.

Ivančić, I., Herak, D., Markušić, S., Sović, I., and Herak, M. (2006), Seismicity of Croatia in the period 2002-2005, Geofizika 23, 87-103.

Kahle, H.-G., Cocard, M., Peter, Y,. Geiger, A., Reilinger, R., Barka, A., and Veis, G. (2000), GPS-derived strain rate field within the boundary zones of the Eurasian, African and Arabian Plates, J. Geophys. Res. 105(B10), 23,353-23,370, doi: 10.1029/2000JB900238.

Kahle, H.-G., Müller, M.V., and Veis, G. (1996), Trajectories of crustal deformation of Western Greece from GPS observations 1989-1994, Geophys. Res. Lett. 23, 677-680.

Kahle, H-G., Straub, C., Reilinger, R., McClusky, S., King, R., Hurst, K., Veis, G., Kastens, K., and Cross, P. (1998), The strain rate field in the eastern Mediterranean region, estimated by repeated GPS measurements, Tectonophysics 294, 237-252.

Kanamori, H., and Brodsky, E. E. (2004), The physics of earthquakes, Rep. Prog. Phys. 67, 1429-1496.

Kowalik, Z., Horrillo, J., Knight, W., and Logan, T. (2008), Kuril Islands tsunami of November 2006: 1. Impact at Crescent City by distant scattering, J. Geophys. Res. 113, C01020, doi:10.1029/2007JC004402.

Kuk, V., Prelogović, E. and Dragičević, I. (2000), Seismotectonically Active Zones in the Dinarides, Geologica Croatica 53, 295-303.

Lavecchia, G., De Nardis, R., Visini, F., Ferrarini, F., and Barbano, M.S. (2007), Seismogenic evidence of ongoing compression in eastern-central Italy and mainland Sicily: a comparison, Boll. Soc. Geol. Ital. (Ital. J. Geosci.) 126, 209–222.

Lawrence, S.R., Tari-Kovačić, V., and Gjukić, B. (1995), Geological evolution model of the Dinarides, Nafta 46, 103-113.

Lorito, S., Tiberti, M. M., Basili, R., Piatanesi, A., and Valensise, G. (2008), Earthquake-generated tsunamis in the Mediterranean Sea: Scenarios of potential threats to Southern Italy, J. Geophys. Res. 113, B01301, doi:10.1029/2007JB004943.

Louvari, E., Kiratzi, A.A., and Papazachos, B.C. (1999), The Cefalonia Transform Fault and its extension to western Lefkada Island (Greece), Tectonophysics 308, 223-236.

Mader, C. L., Numerical modeling of water waves, Los Alamos series in Basic and Applied Sciences (CRC Press, Boca Raton, Florida, 2001), 206 pp.

Mamuzić, P. (1975), Osnovna geološka karta SFRJ, list Šibenik, 1:100000. Inst. geol. istraž., Zagreb (1966), Savezni geol. zavod, Beograd.

Maramai, A., Graziani, L., and Tinti, S. (2007), Investigation on tsunami effects in the central Adriatic Sea during the last century – a contribution, Nat. Hazards Earth Syst. Sci. 7, 15–19.

Markušić, S., Herak, D., Ivančić, I., and Sović, I. (1998), Seismicity of Croatia in the period 1993–1996 and the Ston-Slano earthquake of 1996, Geofizika 15, 83–101.

McClusky, S., Balassanian, S., Barka, A., Demir, C., Ergintav, S., Georgiev, I., Gurkan, O., Hamburger, M., Hurst, K., Kahle, H., Kastens, K., Kekelidze, G., King, R., Kotzev, V., Lenk, O., Mahmoud, S., Mishin, A., Nadariya, M., Ouzounis, A., Paradissis, D., Peter, Y., Prilepin, M., Reilinger, R., Sanli, I., Seeger, H., Tealeb, A., Toksöz, M. N., and Veis, G. (2000), Global Positioning System constraints on plate kinematics and dynamics in the eastern Mediterranean and Caucasus, J. Geophys. Res. 105 (B3), 5695-5719, 10.1029/1999JB900351.

Meletti, C., Galadini, F., Valensise, G., Stucchi, M., Basili, R., Barba, S., Vannucci, G., and Boschi, E. (2008), The ZS9 seismic source model for the seismic hazard assessment of the Italian territory, Tectonophysics 450, 85-108.

Milano, G., Di Giovambattista, R., and Ventura, G. (2005), Seismic constraints on the present-day kinematics of the Gargano foreland, Italy, at the transition zone between the southern and northern Apennine belts, Geoph. Res. Lett. 32, L24308, doi:10.1029/2005GL024604.

Nocquet, J.-M., and Calais, E. (2004), Geodetic measurements of crustal deformation in the Western Mediterranean and Europe, Pure Appl. Geophys. 161, 661–681, doi:10.1007/s00024-003-2468-z.

Okada, Y. (1985), Surface deformation due to shear and tensile faults in a half-space, Bull. Seismol. Soc. Am. 75, 1135–1154.

Okada, Y. (1992), Internal deformation due to shear and tensile faults in a half-space, Bull. Seismol. Soc. Am. 82, 1018-1040.

Olivieri, M., and Scognamiglio, L. (2007), Toward a Euro Mediterranean tsunami warning system: The case of the February 12, 2007, Ml = 6.1 earthquake, Geoph. Res. Lett. 34, L24309, doi:10.1029/2007GL031364.

Papaioannou, Ch. A., and Papazachos, B.C. (2000), Time-independent and time-dependent seismic hazard in Greece based on seismogenic sources, B. Seismol. Soc. Am. 90, 1, 22-33.

Papazachos, B. C. and Dimitriu, P. P. (1991), Tsunamis in and near Greece and their relation to the earthquake focal mechanisms, Natural Hazards 4, 161-170.

Papazachos, B., and Papazachou, C., The earthquakes of Greece (Ziti, Thessaloniki, Greece, 1997).

Papazachos, B.C., Papadimitriou, E.E., Kiratzi, A.A., Papazachos, C.B., and Louvari, E.K. (1998), Fault plane solutions in the Aegean Sea and the sourrounding area and their tectonic implications, Boll. Geof. Teor. Appl. 39, 199-218.

Papazachos, B. C., Papaioannou, C. A., Papazachos, C. B., and Savvaidis, A. S. (1999), Rupture zones in the Aegean region, Tectonophysics 308, 205-221.

Paulatto, M., Pinat, T., and Romanelli, F. (2007), Tsunami hazard scenarios in the Adriatic Sea domain, Nat. Hazards Earth Syst. Sci., 7, 309–325.

Piccinini, D., Chiarabba, C., Augliera, P., and Monghidoro Earthquake Group (M.E.G.) (2006), Compression along the northern Apennines? Evidence from the Mw 5.3 Monghidoro earthquake, Terra Nova 18, 89–94, doi: 10.1111/j.1365-3121.2005.00667.x.

Picha, F.J. (2002), Late orogenic strike-slip faulting and escape tectonics in frontal Dinarides-Hellenides, Croatia, Yugoslavia, Albania, and Greece, Am. Ass. Petroleum Geologists Bull., 86, 1659-1671.

Pirazzoli, P.A., Stiros, S. C., Laborel, J., Laborel-Deguen, F., Arnold, M., Papageorgiou, S., and Morhange, C. (1994), Late-Holocene shoreline changes related to palaeoseismic events in the Ionian Islands, Greece, The Holocene 4, 397-405.

Pondrelli, S., Piromallo, C., and Serpelloni, E. (2004), Convergence vs. Retreat in Southern Tyrrhenian Sea: Insights from kinematics, Geophys. Res. Lett. 31, L06611, doi: 10.1029/2003GL019223.

Pondrelli, S., Salimbeni, S., Ekström, G., Morelli, A., Gasperini, P., and Vannucci, G. (2006), The Italian CMT dataset from 1977 to the present, Phys. Earth Planet. Int. 159, 286-303.

Power, W., Downes, G., and Stirling, M. (2007), Estimation of Tsunami Hazard in New Zealand due to South American Earthquakes, Pure Appl. Geophys. 164, 547–564, doi: 10.1007/s00024-006-0166-3.

Prelogović, E., Aljinović, B., and Bahun, S. (1995), New data on structural relationships in the North Dalmatian area, Geologica Croatica 48, 167–176.

Prelogović, E., Kuk, V., Buljan, R., Tomljenović, B., and Skoko, D. (1999), Recent tectonic movements and earthquakes in Croatia, Proceedings of the Second International Symposium: Geodynamics of Alps-Adria Area by means of Terrestrial and Satellite Methods, Dubrovnik, 255–262.

Prelogović, E., Pribičević, B., Ivković, Ž ., Dragičević, I., Buljan, R., and Tomljenović, B. (2003), Recent structural fabric of the Dinarides and tectonically active zones important for petroleum-geological exploration in Croatia, Nafta 55, 155– 161.

Ridente, D., Fracassi, U., Di Bucci, D., Trincardi, F., and Valensise, G. (2008), Middle Pleistocene to Holocene activity of the Gondola Fault Zone (Southern Adriatic Foreland): deformation of a regional shear zone and seismotectonic implications, Tectonophysics 453, 110-121, doi:10.1016/j.tecto.2007.05.009.

Royden, L., Patacca, E., and Scandone, P. (1987), Segmentation and configuration of subducted lithosphere in Italy: An important control on thrust-belt and foredeep-basin evolution, Geology 15, 714-717.

Scrocca, D. (2006), Thrust front segmentation induced by differential slab retreat in the Apennines (Italy), Terra Nova 18, 154–161.

Scrocca, D., Carminati, E., Doglioni, C. and Marcantoni, D., Slab retreat and active shortening along the centralnorthern Apennines, In Thrust Belts and Foreland Basins: From Fold Kinematics to Hydrocarbon Systems (eds. Lacombe O., Lave' J., Roure F., and Verges J.,) (Frontiers in Earth Sciences, Springer-Verlag, Berlin Heidelberg, Germany 2007) pp. 471–487.

Serpelloni, E., Vannucci, G., Pondrelli, S., Argnani, A., Casula, G., Anzidei, M., Baldi, P., and Gasperini, P. (2007), Kinematics of the Western Africa-Eurasia plate boundary from focal mechanisms and GPS data, Geophys. J. Int. 169, 1180–1200, doi: 10.1111/j.1365-246X.2007.03367.x.

Serpelloni, E., Anzidei, M., Baldi, P., Casula, G., and Galvani, A. (2005), Crustal velocity and strain-rate fields in Italy and surrounding regions: new results from the analysis of permanent and non-permanent GPS networks, Geophys. J. Int. 161, 861-880, doi: 10.1111/j.1365-246X.2005.02618.x.

Skoko, D., Prelogović, E., and Aljinović, B. (1987), Geological structure of the Earth's crust above the Moho discontinuity in Yugoslavia, Geophysical Journal of the Royal Astronomical Society 89, 379– 382.

Smith, W. H. F., and Sandwell, D. T. (1997), Global sea floor topography from satellite altimetry and ship depth soundings, Science 277, 1956-1962.

Soloviev, S. L., Solovieva, O. N., Go, C. N., Kim, K. S., and Shchetnikov, N. A. , Tsunamis in the Mediterranean Sea 2000 B.C.– 2000 A.D., Advances in Natural and Technological Hazard Research (Kluwer Academic Publishers, 2000).

Stiros, S.C., Pirazzoli, P.A., Laborel, J., and Laborel-Deguen, F. (1994), The 1953 earthquake in Cephalonia (Western Hellenic Arc): coastal uplift and halotectonic faulting, Geophys. J. Int. 117, 834-849.

Sulstarova, E., Peçi, V., and Shuteriqi, P. (2000), Vlora-Elbasani-Dibra (Albania) transversal fault zone and its seismic activity, Journal of Seismology 4**,** 117–131.

Tari, V. (2002), Evolution of the northern and western Dinarides: a tectonostratigraphic approach, EGU Stephan Mueller Special Publication Series 1, 223–236.

Tari Kovačić, V., and Mrinjek, E. (1994), The Role Of Paleogene Clastics In The Tectonic Interpretation Of Northern Dalmatia (Southern Croatia), Geologica Croatica 47, 127-138.

Thomson, R. E., Rabinovich, A. B., and Krassovski, M. V. (2007), Double jeopardy: concurrent arrival of the 2004 Sumatra tsunami and storm-generated waves on the Atlantic coast of the United States and Canada, Geophys. Res. Lett. 34, L15607, doi:10.1029/2007GL030685.

Tinti, S., and Armigliato, A. (2003), The use of scenarios to evaluate the tsunami impact in southern Italy, Marine Geology 199, 221-243.

Tinti, S., and Piatanesi, A. (1996), Numerical simulations of the tsunami induced by the 1627 earthquake affecting Gargano, Southern Italy, Journal of Geodynamics 21, 141-160.

Tinti, S., Maramai, A., and Graziani L. (2004), The new catalogue of Italian tsunamis, Natural Hazards 33, 439-465.

Tinti, S., Maramai, A., and Graziani, L. (2007), The Italian Tsunami Catalogue (ITC), Version 2, http://web1.ingv.it:8080/portale_ingv/servizi-e-risorse/cartella-banche-dati/catalogo-tsunami/catalogo-degli-tsunami-italiani.

Valensise, G., Pantosti, D., and Basili, R. (2004), Seismology and Tectonic Setting of the 2002 Molise, Italy, Earthquake, Earthquake Spectra 20, S1, 23-37.

Vannoli, P., Basili, R., and Valensise, G. (2004), New geomorphic evidence for anticlinal growth driven by blind-thrust faulting along the northern Marche coastal belt (central Italy), J. Seismol. spec. vol. 8, 297-312.

Vannucci, G., Pondrelli, S., Argnani, A., Morelli, A., Gasperini, P., and Boschi, E. (2004), An atlas of Mediterranean seismicity, Annals of Geophysics Suppl. to vol. 47, 247-306.

Whitmore, P.M. (2003), Tsunami amplitude prediction during events: a test based on previous tsunamis, Sci. Tsunami Haz. 21, 135–143.

Zerbini, S, Matonti, F, and Doglioni, C. (2006), Crustal movements in northeastern Italy from permanent GPS stations, European Geosciences Union 2006, Geophysical Research Abstracts 8, 06257.

Table 1. Summary of parameters of the Typical Faults shown in **Figure 1**. L: fault length; W: fault down-dip width; D: depth of top edge of fault below sea level. MCE: Maximum Credible Earthquake for the given fault.

	Source Zone	L (km)	W (km)	D (km)	Slip (m)	Strike (deg)	Dip (deg)	Rake (deg)	MCE (M_w)
a	Coastal Croatia	16	7	1	0.6	312	40	110	6.1
	Offshore Croatia	11	6.6	2	0.6	305	45	80	6.0
b	Montenegro	50	20	1	2.5	312	35	82	7.2
c	Albania-N Greece	36.2	16	1	2.0	337	35	96	7.0
d	Northern Apennines	12	8	2.5	0.6	140	30	90	6.1
e	Apulia	34	15	1	0.9	275	80	173	6.7
f	Kefallonia-Lefkada	110	18	3	2.0	27	60	162	7.3

FIGURE CAPTIONS

Figure 1. Tectonic sketch map of the Adriatic basin. The double-headed arrow indicates the floating path of the Typical Faults (see Table 1 for their parameters). a) Coastal and Offshore Croatia; b) Montenegro; c) Albania - Northern Greece; d) Northern Apennines; e) Apulia; f) Kefallonia-Lefkada. Selected major earthquakes discussed in the paper are indicated. The traces of the cross sections in **Figure 2** are also shown.

Figure 2. Cross sections of the main thrust structures. Vertical arrows indicate the position of the active fronts selected for the modeling (see **Figure 1**). a) Dinarides: data taken from Tari-Kovačić and Mrinjek (1994); Tari (2002) and Ivančić et al. (2006); b) Montenegro: data taken from Dragašević (1983) and Picha (2002); c) Northern Albania offshore: section modified after Graham Wall et al. (2006); d) Northern Apennines: section redrawn after Scrocca et al. (2007).

Figure 3. Diagram of tsunami impact along the Italian coastlines of the Adriatic Sea following earthquakes generated by the a) Croatia SZ, b) Montenegro SZ, c) Albania - Northern Greece SZ, d) Northern Apennines SZ, e) Apulia SZ, and f) Kefallonia-Lefkada SZ. The profiles show maximum (black), average (blue) and average plus one standard deviation (green) of the HMAXs (maximum water height above the mean sea level) aggregated for each SZ. Horizontal scales are distances in kilometers: see **Figure 4** for locating the diagram relative to the coastline. Vertical scales are water heights in meters. Yellow, orange and red in the background show the *marine*, *land* and *severe land threat* levels respectively (see text).

Figure 4. Combined threat levels posed by all SZs considered in this study (except for the Hellenic Arc), color-coded as in **Figure 3,** and progressive distance (in km) along the target coastlines used for displaying the modeling results. This map is intended for use in conjunction with **Figures 3, 6** and **7**.

Figure 5. Map of the maximum water height above the mean sea level in the simulation domain, for some selected fault positions in two different SZ: a) and b) are generated by two faults in the Montenegro SZ; c) is generated by a fault in the Albania - Northern Greece SZ; d) is generated by a fault in the Kefallonia-Lefkada SZ.

Figure 6. Diagram of tsunami impact along the Italian coastlines of the Adriatic Sea: aggregated HMAXs (maximum water height above the mean sea level) from the Hellenic Arc SZ. Line colors and threat levels in the background as in **Figure 3**.

Figure 7. Synoptic diagram of tsunami impact shown as aggregated HMAXs maximum for each source zone. Black: Kefallonia-Lefkada; magenta: Albania - Northern Greece; blue: Montenegro; brown: Croatia; cyan: Northern Apennines; green: Apulia. The maximum HMAXs produced by the Hellenic Arc SZ is shown in gray. Threat levels in the background as in **Figure 3**, water heights are above the mean sea level.

Figure 8. Snapshots of the tsunami wave height for two selected faults: a) in the Albania – Northern Greece SZ; b) in the Montenegro SZ.

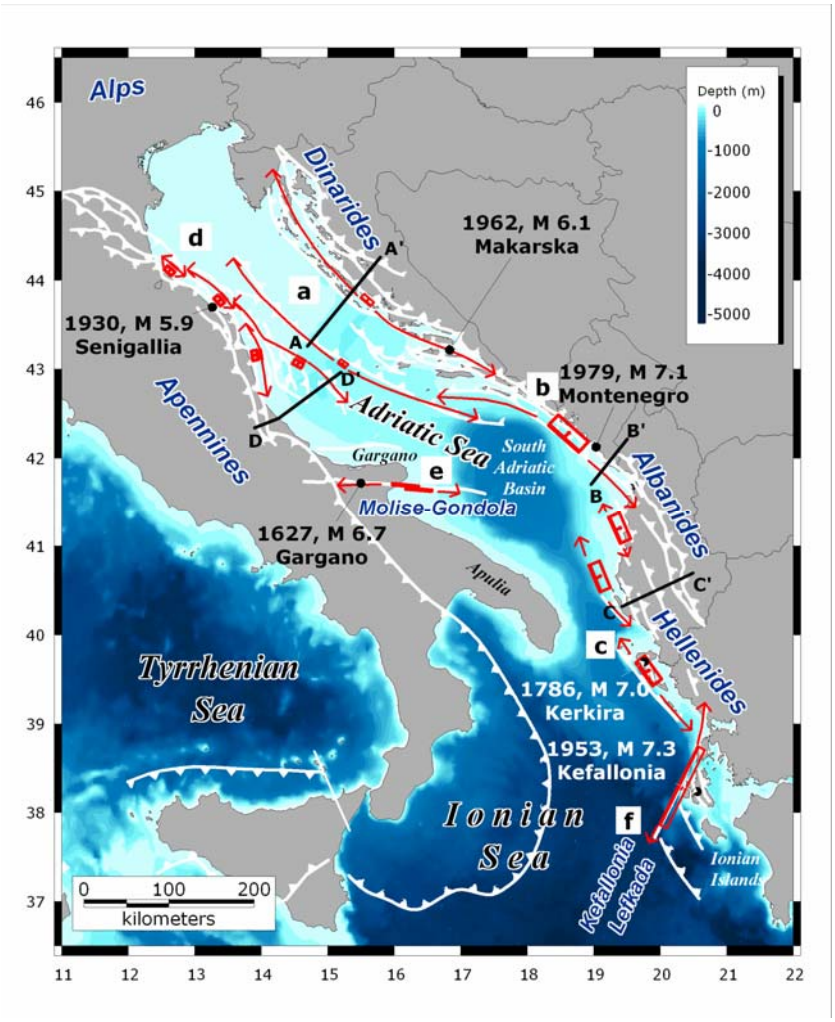
Alps
Dinarides
Apennines
Albanides
Hellenides
Adriatic Sea
South Adriatic Basin
Tyrrhenian Sea
Ionian Sea
Gargano
Molise-Gondola
Apulia
Kefallonia
Lefkada
Ionian Island
1962, M 6.1
Makarska
1930, M 5.9
Senigallia
1979, M 7.1
Montenegro
1627, M 6.7
Gargano
1786, M 7.0
Kerkira
1953, M 7.3
Kefallonia
a
b
c
d
e
f
A
A'
B
B'
C
C'
D
D'
Depth (m)
0
-1000
-2000
-3000
-4000
-5000
0
100
200
kilometers
46
45
44
43
42
41
40
39
38
37
11
12
13
14
15
16
17
18
19
20
21
22

Figure 1

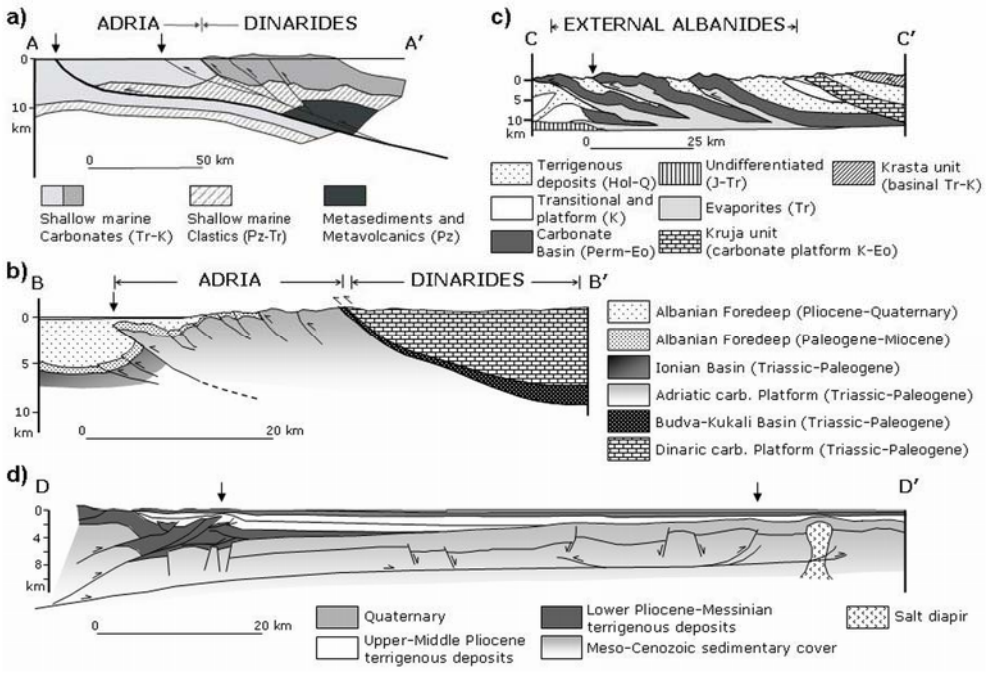
a)
ADRIA
DINARIDES
A
A′
0
10
km
0
50 km
Shallow marine Carbonates (Tr-K)
Shallow marine Clastics (Pz-Tr)
Metasediments and Metavolcanics (Pz)
c)
EXTERNAL ALBANIDES
C
C′
0
5
10
km
0
25 km
Terrigenous deposits (Hol-Q)
Undifferentiated (J-Tr)
Krasta unit (basinal Tr-K)
Transitional and platform (K)
Evaporites (Tr)
Carbonate Basin (Perm-Eo)
Kruja unit (carbonate platform K-Eo)
b)
B
ADRIA
DINARIDES
B′
0
5
10
km
0
20 km
Albanian Foredeep (Pliocene-Quaternary)
Albanian Foredeep (Paleogene-Miocene)
Ionian Basin (Triassic-Paleogene)
Adriatic carb. Platform (Triassic-Paleogene)
Budva-Kukali Basin (Triassic-Paleogene)
Dinaric carb. Platform (Triassic-Paleogene)
d)
D
D′
0
4
8
km
0
20 km
Quaternary
Upper-Middle Pliocene terrigenous deposits
Lower Pliocene-Messinian terrigenous deposits
Meso-Cenozoic sedimentary cover
Salt diapir

Figure 2

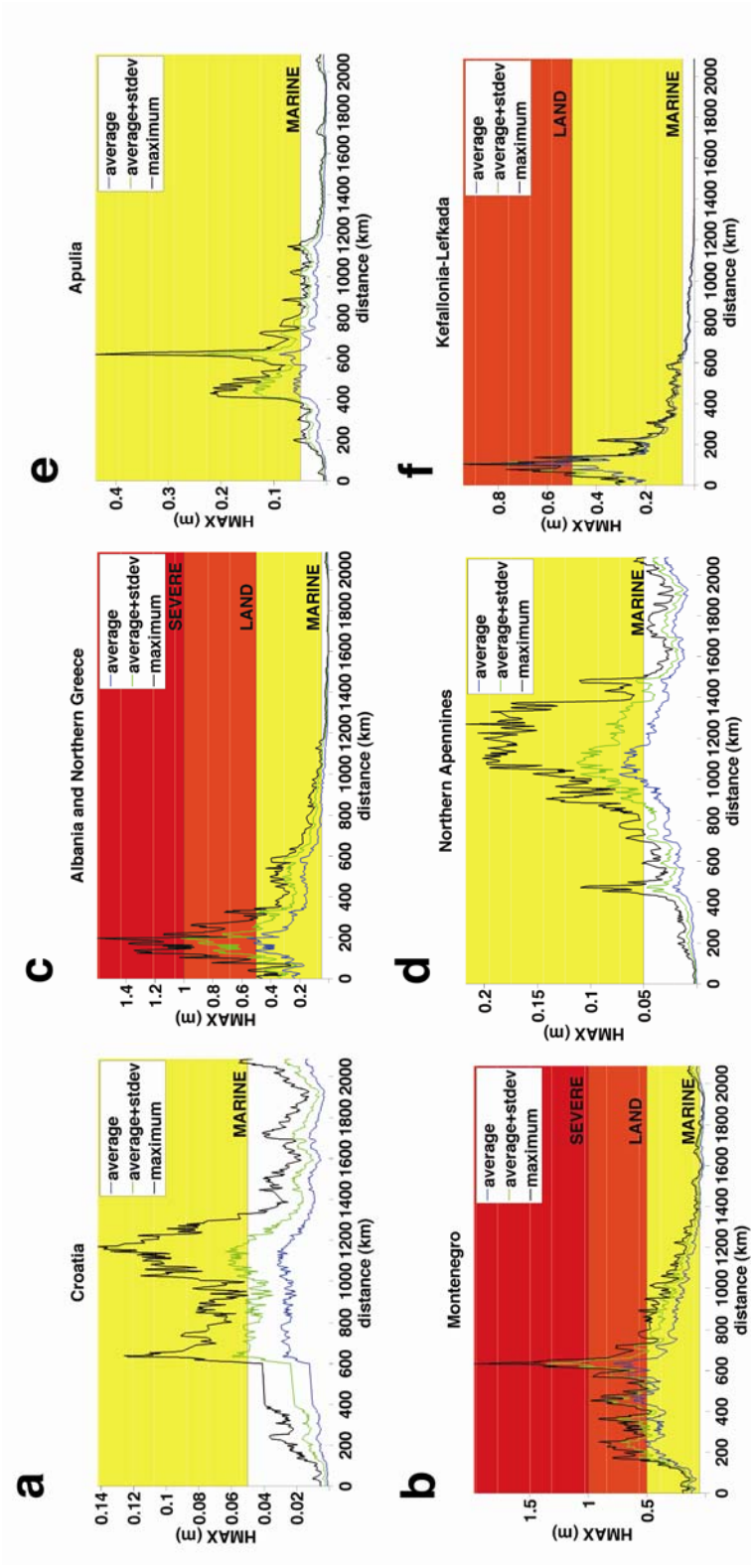
a
Croatia
b
Montenegro
c
Albania and Northern Greece
d
Northern Apennines
e
Apulia
f
Kefallonia-Lefkada
average
average+stdev
maximum
MARINE
LAND
SEVERE
HMAX (m)
distance (km)

Figure 3

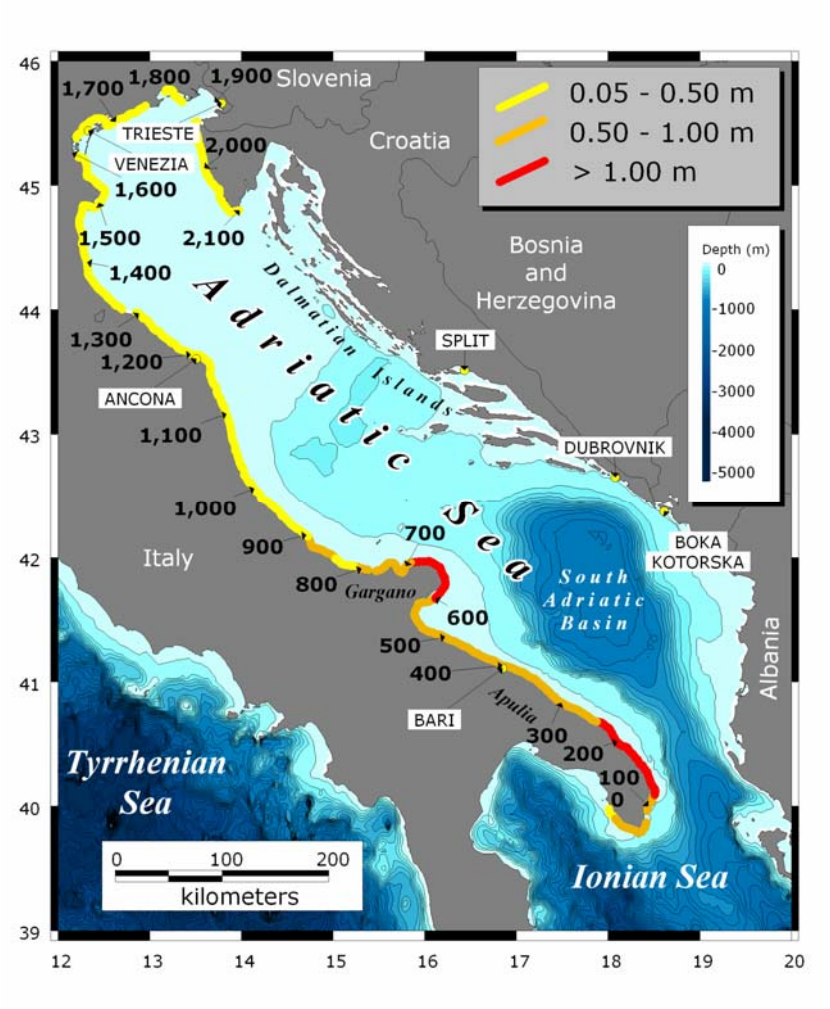
0.05 - 0.50 m
0.50 - 1.00 m
> 1.00 m
Depth (m)
0
-1000
-2000
-3000
-4000
-5000
Slovenia
Croatia
Bosnia and Herzegovina
Italy
Albania
Adriatic Sea
Dalmatian Islands
South Adriatic Basin
Gargano
Apulia
Tyrrhenian Sea
Ionian Sea
TRIESTE
VENEZIA
ANCONA
SPLIT
DUBROVNIK
BOKA KOTORSKA
BARI
1,700
1,800
1,900
2,000
1,600
1,500
2,100
1,400
1,300
1,200
1,100
1,000
900
800
700
600
500
400
300
200
100
0
0 100 200
kilometers
46
45
44
43
42
41
40
39
12
13
14
15
16
17
18
19
20

Figure 4

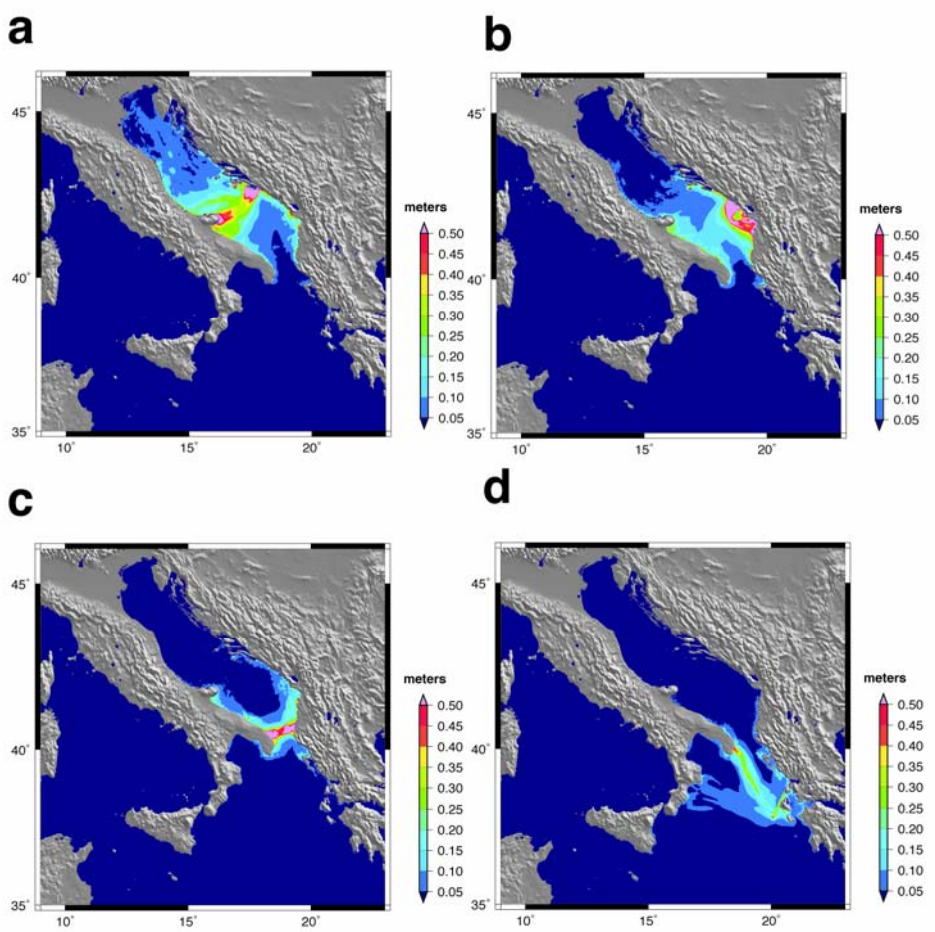
a
b
c
d
meters
0.50
0.45
0.40
0.35
0.30
0.25
0.20
0.15
0.10
0.05
45°
40°
35°
10°
15°
20°

Figure 5

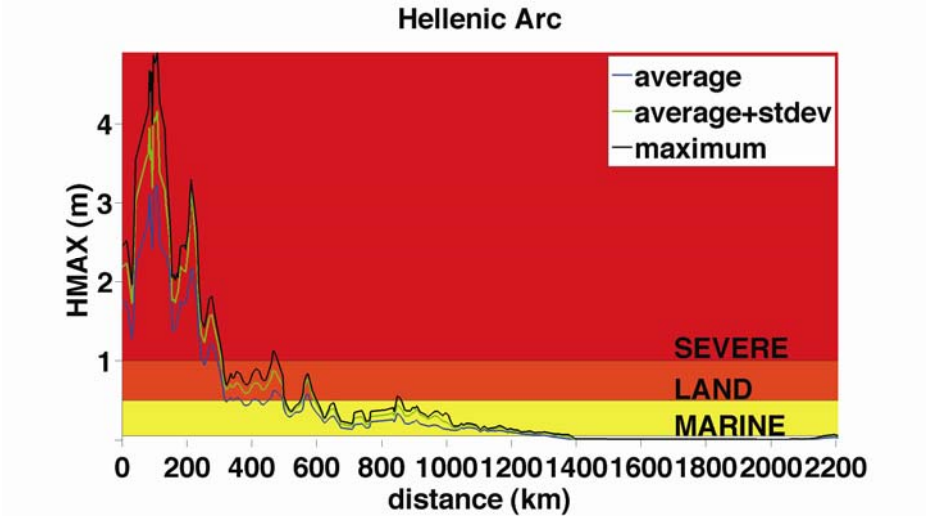

Figure 6

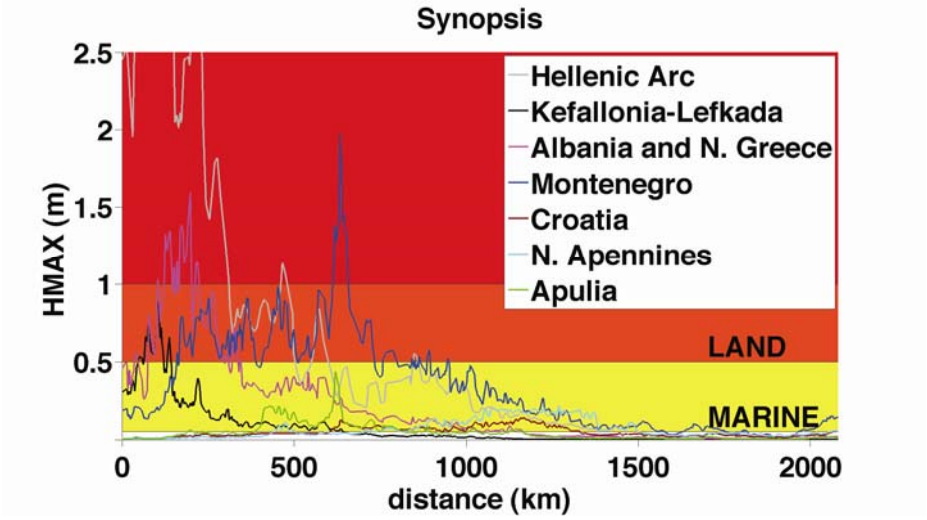

Figure 7

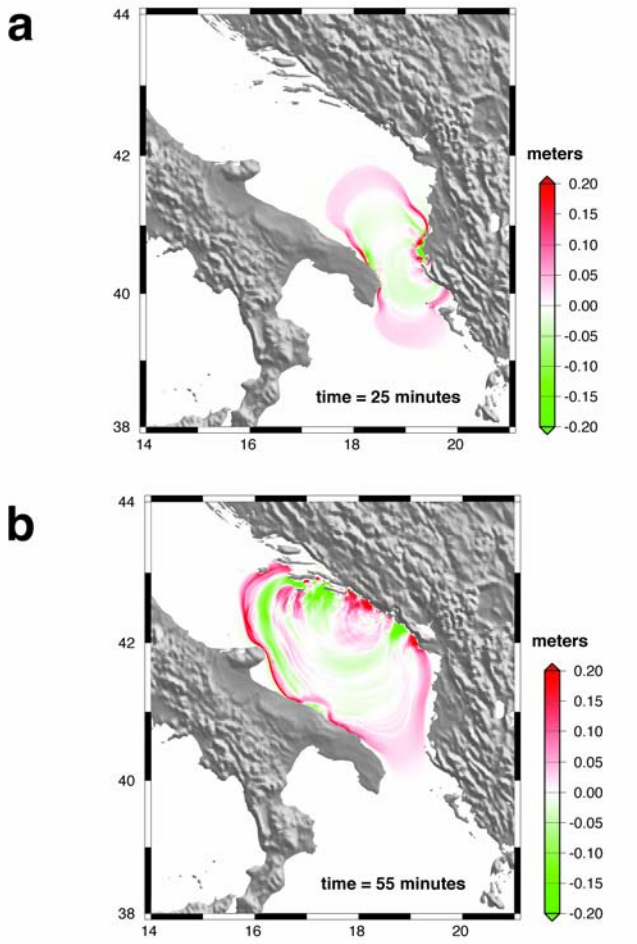
a
b
meters
0.20
0.15
0.10
0.05
0.00
-0.05
-0.10
-0.15
-0.20
time = 25 minutes
time = 55 minutes
44
42
40
38
14
16
18
20

Figure 8